New Horizons in Earth Reinforcement – Otani, Miyata & Mukunoki (eds)
© 2008 Taylor & Francis Group, London, ISBN 978-0-415-45775-0

Modelling fibre reinforced sand

A. Diambra, E. Ibraim & D.M. Wood
Department of Civil Engineering, University of Bristol, Bristol, United Kingdom

A. Russell
School of Civil and Environmental Engineering, University of New South Wales, Sydney, Australia
(formerly Department of Civil Engineering, University of Bristol)

ABSTRACT: Results of triaxial compression tests for a reinforced sand show that the effectiveness of fibres as a reinforcing agent depends largely on their concentration as well as their orientation with respect to tensile strains which develop. In this paper a modelling approach for implementing the effects of fibre reinforcement into a constitutive model is presented. Application of the approach is demonstrated using an example where it is assumed that the soil stress:strain behaviour may be described by the elastic-perfectly plastic Mohr-Coulomb model. The modelling approach is based on the rule of mixtures in which the stresses in the fibres and the stresses in the sand matrix are superposed according to their volumetric fraction. A fibre stiffness matrix is defined in which it is assumed that fibres are working in their elastic domain. It accounts for fibre concentration and fibre orientation distribution. Drained triaxial compression test results for reinforced sand are presented as are model outputs. The model simulates the major characteristic features such as a monotonically increasing shear stress with increasing shear strain.

1 INTRODUCTION

Mixing sands with random discrete flexible fibres increases their strength and alters their deformation characteristics. Reinforced sands of this type are gaining acceptance by engineers as a cost effective and strong geomaterial.

Most research in this area has focused on the experimental stress:strain behaviour of reinforced sands (Michałowski & Čermák 2003 and Heineck et al. 2005 among others). There have been only a few attempts to model the constitutive behaviour of reinforced sands. Most were limited to the determination of the shear strength (Zornberg 2002 and Michałowski & Čermák 2002, among others). However, there are a few examples of modelling the stress:strain behaviour. The first (Villard et al. 1990) used the principle of superposition, where the stress:strain behaviour of soil and fibres were treated separately. Ding & Hargrove (2006) proposed a nonlinear stress:strain relationship for reinforced soil by using a volumetric homogenization technique. However, none of these models are able to account for non-uniform fibre orientation distributions.

In this research the fibre reinforced soil is treated as a composite with a stress:strain behaviour that obeys the rule of mixtures. The stiffnesses of the fibres and sand are defined separately and then superposed according to their volumetric fraction. Emphasis is placed on accounting for the concentration and orientation distribution of the fibres in a systematic way, and how the corresponding fibre stiffness matrix may be combined with any sand stiffness matrix. Application of the modelling approach is demonstrated using the simple Mohr-Coulomb elastic-perfectly plastic model for the sand, although more complex models for sand could be used in the same way.

A range of stress–strain behaviours of the composite are presented and compared to those observed from triaxial tests. The modelling approach enables simulation of the major characteristic features such as a monotonically increasing shear stress with increasing shear strain. It is also shown that the model outputs are very sensitive to the fibre orientation distribution.

2 A MODELLING FRAMEWORK

2.1 *Rule of mixtures*

The rule of mixtures may be used when studying the stress:strain behaviour of a composite material. Each component of the composite satisfies its own constitutive law. When each component is homogeneously distributed throughout the composite, their individual

contributions to the overall composite behaviour are linked to their volumetric fractions. It follows that, for a reinforced sand, the general definitions for the stress and strain of a composite, expressed in terms of stresses and strains of the sand matrix and fibres, are:

$$\sigma = \sigma_m v_m + \sigma_f v_f \tag{1}$$

and

$$\varepsilon = \varepsilon_m v_m + \varepsilon_f v_f \tag{2}$$

where $\sigma, \sigma_m, \sigma_f, \varepsilon, \varepsilon_m$ and ε_f are the stresses and strains in the composite, matrix and fibres, respectively. The concentration factors v_m and v_f (for the matrix and the fibres, respectively) are defined as:

$$v_m = \frac{V_m}{V} = \frac{V - V_f}{V}, \quad v_f = \frac{V_f}{V} \tag{3}$$

where V, V_m and V_f are the volumes of the composite, matrix and fibres, respectively. Notice that concentration factors are related by:

$$v_m + v_f = 1 \tag{4}$$

These definitions for the concentration factors are universally accepted when each component of the composite behaves elastically. Even when different components behave plastically it is common for researchers using the rule of mixtures to adopt the same definitions as for the elastic range. Examples include Dvorak & Bahei-El-Din (1987) and Voyaiadjis & Thiagarajan (1995) for reinforced metal-matrix composites, Car et al. (2000) for anisotropic elastoplastic behaviour for fibre reinforced material at large strains, Luccioni (2006) for fibre-reinforced laminates, Ortiz & Popov (1982) when model the behaviour of concrete as a composite of mortar and aggregates, and Villard et al. (1990) and di Prisco & Nova (1993) when modelling fibre reinforced soils. However, there are a few exceptions. For a reinforced metal-matrix composite Dvorak & Bahei-El-Din. (1982) determined instantaneous concentration factors to evaluate the instantaneous stresses in the matrix and in the fibres in the plastic region.

One of two main hypotheses must be assumed when using the rule of mixtures: Voigt's hypothesis or Reuss's hypothesis. The former generally assumes that the strain fields in the composite coincide with those of its components:

$$\varepsilon = \varepsilon_m = \varepsilon_f \tag{5}$$

In the later an equality of stresses is assumed:

$$\sigma = \sigma_m = \sigma_f \tag{6}$$

To maintain simplicity in the formulations that follow it is supposed that sliding between sand grains and fibres is absent, fibres only act in tension and elastically and Voigt's hypothesis applies.

A very minor modification to the classical rule of mixtures was also made for simplicity. More specifically, the concentration factors are defined as the (slightly approximate) expressions:

$$v_m = 1 \quad \text{and} \quad v_f = \frac{V_f}{V} \tag{7}$$

which is reasonable since the volume of the fibres is very small compared to the volume of the composite, i.e. $V_f << V$. The final form of the stress:strain relationship for the reinforced soil, when expressed incrementally, is:

$$\dot{\sigma} = \dot{\sigma}_m + v_f \dot{\sigma}_f = [M_s]\dot{\varepsilon} + v_f [M_f]\dot{\varepsilon} \tag{8}$$

where M_s is the stiffness matrix for the sand and M_f is the stiffness matrix for the fibres.

2.2 *Modelling fibres behaviour*

2.2.1 *Single fibre*

In reinforced composites fibres are embedded in the sand matrix and according to the Voigt's hypothesis the deformation in the fibres coincides with the deformation in the sand. Thus the entity of deformation in a single fibre depends on its orientation. Also, assuming an elastic behaviour for the fibres, even the entity of the stress in the fibre depends on fibre orientation as will now be shown. Considering conventional triaxial conditions, the following relationship between the strains at any angle θ from the horizontal (ε_θ) and the principal strains (ε_1 in vertical direction and ε_3 in horizontal direction) can be easily obtained:

$$\varepsilon_\theta = \varepsilon_1 \sin^2(\theta) + \varepsilon_3 \cos^2(\theta) \tag{9}$$

The stress carried by an elastic fibre oriented by an angle θ from the horizontal is then:

$$\sigma_\theta = E_f \varepsilon_\theta \tag{10}$$

and it is possible to derive the contribution of a single fibre to the principal stresses, $\sigma_{1f}(\theta)$ and $\sigma_{3f}(\theta)$, by decomposing σ_θ to give:

$$\sigma_{1f}(\theta) = \sigma_\theta \sin^2(\theta) \tag{11}$$

$$\sigma_{3f}(\theta) = \sigma_\theta \cos^2(\theta)/2 \tag{12}$$

In expanded form these can be rewritten as:

$$\sigma_{1f}(\theta) = E_f\left(\varepsilon_1 \sin^4(\theta) + \varepsilon_3 \cos^2(\theta)\sin^2(\theta)\right) \tag{13}$$

$$\sigma_{3f}(\theta) = E_f \frac{\left(\varepsilon_1 \sin^2(\theta)\cos^2(\theta) + \varepsilon_3 \cos^4(\theta)\right)}{2} \tag{14}$$

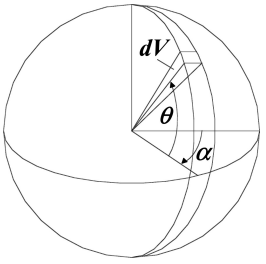

Figure 1. Spherical coordinates used on the definition of the fibre orientation distribution.

2.2.2 *Agglomerate of fibres*

A procedure similar to the one proposed by Zhu et al. (1994) for the determination of the strength of short-fibre reinforced metal-matrix has been used here. Fibres have a non-uniform orientation distribution, and using the spherical coordinates shown in Figure 1, a general fibre orientation distribution function $\rho(\theta)$ is now introduced. $\rho(\theta)$ represents the volumetric concentration of fibres in an infinitesimal volume dV (Fig. 1) having an orientation of angle θ above the horizontal and its main property has to be:

$$\overline{\rho} = \frac{1}{V}\int_V \rho(\theta)\mathrm{d}V \tag{15}$$

where V is the volume of the reference sphere (made of the composite material) shown in Figure 1 and $\overline{\rho}$ is the average fibre concentration defined by:

$$\overline{\rho} = V_f / V \tag{16}$$

According to its definition, $\rho(\theta)$ is the concentration factor v_f representing the contribution of fibres within the composite which have an orientation of θ above the horizontal plane. Expressions for the overall contribution of fibres within the composite in the directions of the principal stresses can then be obtained by integration using the two expressions:

$$\sigma_{f1} = \frac{1}{V}\int_V \rho(\theta)\sigma_{1f}(\theta)\mathrm{d}V \tag{17}$$

$$\sigma_{f3} = \frac{1}{V}\int_V \rho(\theta)\sigma_{3f}(\theta)\mathrm{d}V \tag{18}$$

If the orientation distribution is symmetrical with respect to the horizontal plane, (17) and (18) can be expanded to give:

$$\sigma_{f1} = \frac{E_f}{2}\left(\varepsilon_1\int\rho(\theta)\sin^4(\theta)\cos(\theta)\mathrm{d}\theta + \varepsilon_3\int\rho(\theta)\cos^3(\theta)\sin^2(\theta)\mathrm{d}\theta\right) \tag{19}$$

$$\sigma_{f3} = \frac{E_f}{4}\left(\varepsilon_1\int\rho(\theta)\sin^2(\theta)\cos^3(\theta)\mathrm{d}\theta + \varepsilon_3\int\rho(\theta)\cos^5(\theta)\mathrm{d}\theta\right) \tag{20}$$

It must now be considered that fibres can only contribute to the stresses acting on the composite by acting in tension. According to Mohr's circle for deformation, the direction of zero strain is:

$$\theta_0 = \arctan\sqrt{-\frac{\varepsilon_3}{\varepsilon_1}} \tag{21}$$

and the integrations in (19) and (20) should only be performed within the limits $0 \le \theta \le \theta_0$. It follows that the concentration factor multiplied by the stiffness matrix for the fibres, in terms of principle stresses, is:

$$v_f\left[M_f\right] = E_f\begin{bmatrix} \int_0^{\theta_0}\rho(\theta)\cos(\theta)\sin^4(\theta)\mathrm{d}\theta & \int_0^{\theta_0}\rho(\theta)\cos^3(\theta)\sin^2(\theta)\mathrm{d}\theta \\ \frac{1}{2}\int_0^{\theta_0}\rho(\theta)\cos^3(\theta)\sin^2(\theta)\mathrm{d}\theta & \frac{1}{2}\int_0^{\theta_0}\rho(\theta)\cos^5(\theta)\mathrm{d}\theta \end{bmatrix} \tag{22}$$

2.3 *Modelling sand*

A simple elastic-perfectly plastic Mohr-Coulomb model has been employed for sand. Considering a formulation in the principal directions, in the elastic region the increments of the principal effective stresses are related to the increments of strains through Young's modulus E and the Poisson's ratio μ:

$$\begin{bmatrix}\dot{\sigma}'_1 \\ \dot{\sigma}'_3\end{bmatrix} = \frac{E}{(1+\mu)(1-2\mu)}\begin{bmatrix}1-\mu & 2\mu \\ \mu & 1\end{bmatrix}\begin{bmatrix}\dot{\varepsilon}'_1 \\ \dot{\varepsilon}'_3\end{bmatrix} \tag{23}$$

Yielding occurs when the following relation is satisfied:

$$\dot{\sigma}'_1 = \frac{1+\sin(\varphi)}{1-\sin(\varphi)}\dot{\sigma}'_3 \tag{24}$$

where φ is the friction angle of sand and beyond first yield the relationship between principal strains is:

$$\dot{\varepsilon}_3^p = -\frac{1+\sin(\psi)}{2(1-\sin(\psi))}\dot{\varepsilon}_1^p \tag{25}$$

where ψ is the dilation angle of the sand.

3 APPLICATION

Application of the model will now be demonstrated and outputs will be compared to results of conventional drained triaxial tests performed on Hostun RF(S28) sand reinforced with Loksand type polypropylene fibres. Specimens 70 mm high and 70 mm diameter were prepared with the moist tamping technique in three different layers and a detailed explanation of the formation procedure is given in Diambra et al. (2007). Hostun RF(S28) sand is a fine sand with

Table 1. Details of Loksand™ fibres.

Weight (Denier)	Tensile strength (MPa)	Specific gravity	Elongation at break	Moisture regain
50	225	0.91	160%	<0.1%

mean grain size $D_{50} = 0.32$ mm, coefficient of uniformity $C_u = 1.70$, coefficient of gradation $C_g = 1.1$, specific gravity $G_s = 2.65$ and minimum and maximum void ratios $e_{min} = 0.62$ and $e_{max} = 1.00$, respectively (Ibraim 1998). Loksand discrete polypropylene crimped fibres have a length $l_f = 35$ mm and are of circular cross section with diameter $d_f = 0.1$ mm. Other physical properties of Loksand^{TM} fibres are reported in Table 1. Results of triaxial tests with two different initial void ratios (e) of 0.9 and 1.0 (which respectively correspond to relative densities of $D_r = 0\%$ and 26%) and differrent fibre contents ($\bar{\rho} = 0.43\%$, 0.87% and 1.30%) have been selected here for comparisons with the model outputs. The σ'_3 of the tests was 100 kPa.

3.1 *Parameters for fibres*

Modelling fibre behaviour requires definition of the elastic modulus (E_f) and the orientation distribution of the fibres. E_f was determined experimentally by performing a number of tension tests on the fibres. Using a machine with low precision, the results revealed an approximate value of $E_f = 600$ MPa. As will be illustrated later this leads to a reasonable fit between model outputs and experimental data. Fibre orientation distribution for specimens used in the experimental work was determined through an experimental procedure reported in Diambra et al. (2007) and it was found that the fibres mostly had a near horizontal orientation. The form of fibre orientation distribution proposed by Michałowski & Čermák (2002) was used:

$$\rho(\theta) = \overline{\rho}\left(A + B\left|\cos^n \theta\right|\right) \tag{26}$$

and the parameters A, B and n defining the orientation distribution were calibrated to be $A = 0$, $n = 5$ and $B = 2.04$. Difficulties were encountered in the integration of the fibre stiffness matrix when (26) was implemented so a slightly modified orientation distribution function $\rho(\theta)$ was used in this research. The new function for $\rho(\theta)$ is:

$$\rho(\theta) = \overline{\rho}\,\frac{2ab^2\left|\cos(\theta)\right|}{\cos(\theta)^2(b^2 - a^2) + a^2} \tag{27}$$

where $a = 1.02$ and $b = 0.46$ were determined by forcing equality in (26) and (27) at $\theta = 0$ and by satisfying (15). The similarity between the two orientation distribution functions is illustrated in Fig. 2.

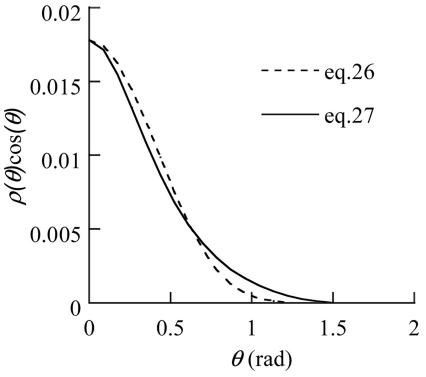

Figure 2. Comparison between the assumed orientation distribution function in eq. 26 and eq. 27.

3.2 *Parameters for sand*

Only a few parameters are needed for the definition of the simple Mohr-Coulomb model. Parameters which give as reasonable fit between model outputs and experimental data include $E = 3600$ kPa, $\mu = 0.3$ and $\phi = 36°$ and were found by trial and error. A value of $\psi = 0°$ was assumed and the appropriateness of this is discussed later.

3.3 *Results and discussion*

Figures 3 and 4 show the drained triaxial test results and model simulations in the $q \sim \varepsilon_q$ plane, where $q = \sigma_1 - \sigma_3$ and $\varepsilon_q = 2(\varepsilon_1 - \varepsilon_3)/3$ are the usual triaxial shear stress and shear strain, respectively. In qualitative terms the model adopted here reproduces the stress:strain response for the reinforced sand quite well. The difference between experimental results and model outputs is mainly due to the simple elastic-perfectly plastic model's inability to account for the non-linearity of unreinforced sand behaviour, especially at small strains. The use of more complex models which capture this non-linearity would result in smoother simulated curves and a better match between experimental data and simulation.

More specifically, the experimental stress:strain responses include an initial non-linear part followed by a linear part that does not flatten with increasing shear strain. The initial non-linear part is largely unaffected by the presence of fibres and the initial sections of the model outputs exhibit this characteristic also. In these initial sections the fibre contribution to the composite behaviour is quite small, which is not surprising as ε_3 is also small, preventing the fibres from elongating and mobilising large tensile forces. At larger shear

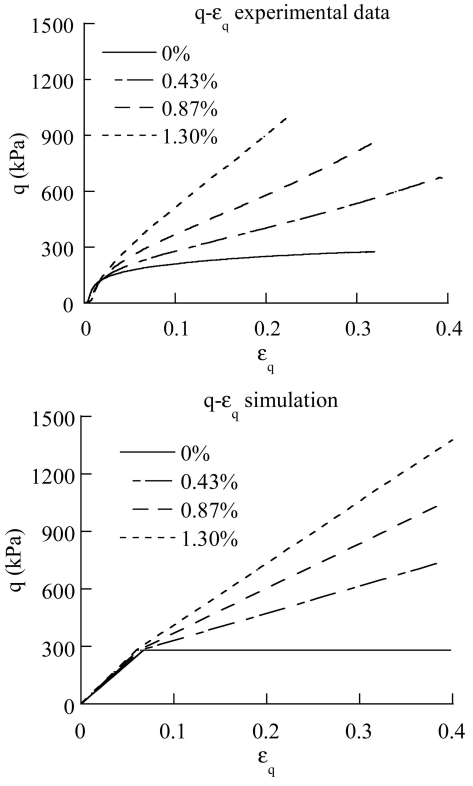

Figure 3. Experimental drained conventional triaxial tests and model simulation for void ratio $e = 1.0$ and cell pressure $\sigma_3' = 100$ kPa. (legend expresses initial fibre content).

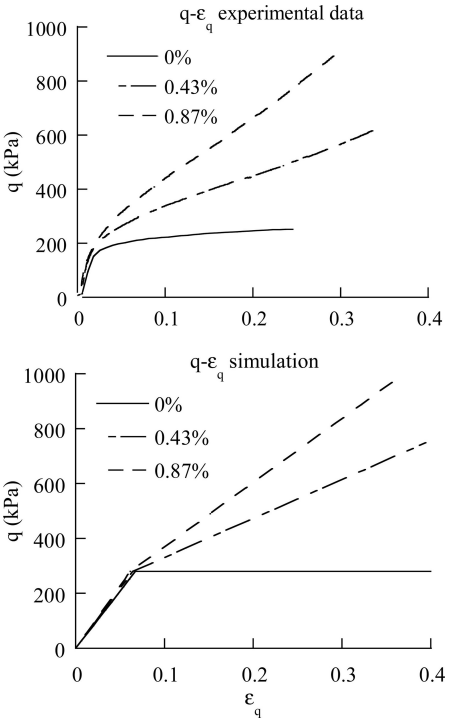

Figure 4. Experimental drained conventional triaxial tests and model simulation for void ratio $e = 0.9$ and cell pressure $\sigma_3' = 100$ mkPa. (legend expresses initial fibre content).

strains ε_3 goes into tension and the shear stress supported by the composite increases, apparently without limit. Fibres go into more and more tension as shear strain is increased. A plausible explanation for this is that, within the range of strains considered, tension is not released due to the fibres breaking, slipping or 'pulling out' of the composite.

The model captures this general behaviour, and the assumptions that fibres are working within their elastic range without slipping seem reasonable. In fact, careful examination of the fibres at the end of the triaxial tests showed no signs of fibre breakage or plastic deformation. In short, for the conventional triaxial test load path, fibres increase the confinement on the sand matrix as shear strain increases, allowing the sand to support greater deviatoric stresses. However, at larger shear strains, the tension in the fibres may be released, for example by breakage, and suppress the increase in deviatoric stress.

The fibre orientation distribution has a major influence on the behaviour of the composite. For the samples prepared here 97% of fibres were orientated within 45° of the horizontal plane (Diambra et al. 2007). This anisotropic fibre orientation distribution results in an anisotropic behaviour of the composite.

Any tendency for ε_3 to decrease (go into tension) is counteracted by a large amount of resistive tension developing in the fibres. If the orientation distribution was isotropic then the effectiveness of the fibres to increase the deviatoric stress supported by the composite will be greatly reduced for the conventional triaxial test load path, as shown by the results of the simulations in Figure 5. Results on samples reinforced with fibres uniformly orientated were not available for the analysed tests, but results published in literature (e.g. Michałowski & Čermák 2002) demonstrate the same influence of fibre orientation as predicted by the proposed model.

The modelling approach outlined above is quite versatile since any fibre orientation distribution can be implemented. Also, the evolution of the effectiveness of the fibres as the sample changes shape, linked to the variation of θ_0 in the integration, is readily accommodated. Furthermore, through minor changes of the framework presented here, different assumptions can be made on the constitutive behaviour of the fibres, such as including a non-linear elasticity or a pull out mechanism between fibres and the sand matrix.

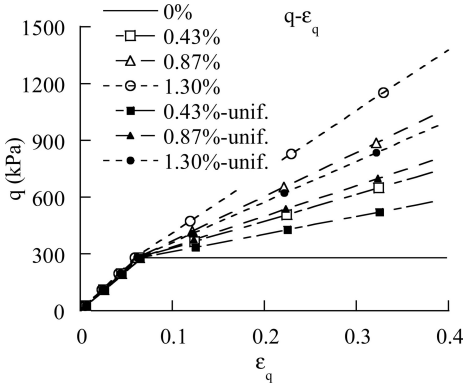

Figure 5. Model simulations for the determined fibre orientation distribution and for an assumed uniform orientation distribution for void ratio $e = 1.0$ and cell pressure $\sigma'_3 = 100$ kPa (legend expresses initial fibre content and fibre orientation).

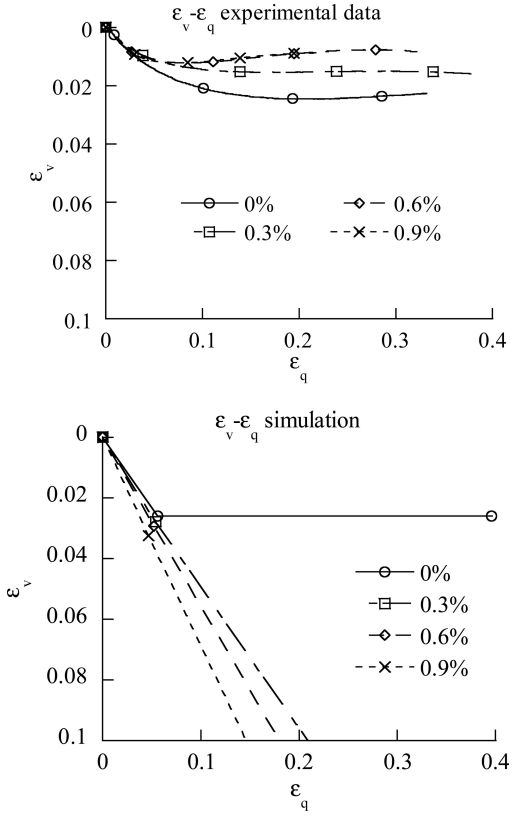

Figure 6. Experimental drained conventional triaxial tests and model simulation for void ratio $e = 1.0$ and cell pressure $\sigma'_3 = 100$ kPa. (legend expresses initial fibre content).

Only poor simulations of the volumetric behaviour were achieved for the assumed $\psi = 0°$ (Fig.6). Experimental results showed that the reinforced sand exhibits a more dilative behaviour than the unreinforced sand and the model is unable to capture this behaviour when using constant dilation angle, irrespective of its value. Further research is in progress to achieve a better understanding of this phenomenon and a better simulation of the experimental data.

4 CONCLUSIONS

A simple modelling approach for fibre reinforced sand has been presented, based on the rule of mixtures. Its application was demonstrated using a simple sand model, and model outputs for the composite exhibit key features that were also observed in triaxial test results. Discrepancies between simulation and experimental results can be attributed to the simplicity of basic sand model and the assumed dilatency relationship. A better simulation would be obtained by adopting a more complex model that captures the non-linear behaviour.

The modelling approach permits the use of any fibre orientation distribution function. It also accounts for the evolution of fibre orientation as the composite deforms.

In any case, the main objective of this work – to outline a very simple modelling tool for fibre reinforced sand – has been met. Furthermore, the very simple model outlined can easily be implemented into a numerical analysis.

REFERENCES

Car, E., Oller, S. & Oñate, E. 2000. An anisotropic elasto-plastic constitutive model for large strain analysis of fiber reinforced composite materials. *Computer methods in applied mechanics engineering* 185: 245–277

di Prisco, C. & Nova, R. 1993 A constittuitve model for soil reinforced by continuous *threads. Geotexiles and Geomembranes* 12:161–178

Diambra, A., Russell, A.R., Ibraim, E. & Muir Wood, D. 2007, Determination of fibre orientation distribution in reinforced sand. *Geotechnique (in press)*

Ding, D. & Hargrove, S.K. 2006. Nonlinear stress-strain relationship of soil reinforced with flexible geofibers. *Journal of Geotechnical & Geoenvironmental Engineering* 132(6): 791–794

Dvorak, G.K. & Bahei-El-Din, Y.A. 1982. Plasticity analysis of fibrous composites. *Journal of applied mechanics* 49: 327–335

Dvorak, G.K. & Bahei-El-Din, Y.A. 1987. A bimodal plasticity theory of fibrous composite materials. *Acta Mechanica* 69: 219–241

Heineck, C.S., Consoli, N.C. & Coop, M.R. 2005. Effect of microreinforcement of soils from very small to large shear strains. *Journal of Geotechnical & Geoenvironmental Engineering* 131(8):1024–1033

Ibraim, E. 1998. Différents aspects du comportement des sables à partir d'essais triaxiaux: des petites déformations à la liquéfaction statique. *PhD thesis*, ENTPE Lyon

Luccioni, B.M. 2006. Constitutive model for fiber-reinforced composite laminates. *Journal of applied mechanics* 73: 901–910

Marakova, I.S. & Saraev, L.A. 1990. Theory of elastic-plastic deformation of randomly reinforced composite materials. *Journal of applied mechanics and technical physics* 32(5): 768–772

Michałowski, R.L. & Čermák, J. 2002. Strength anisotropy of fiber-reinforced sand. *Computers and Geotechnics* 29:279–299

Michałowski, R.L. & Čermák, J. 2003. Triaxial compression of sand reinforced with fibers. *Journal of Geotechnical & Geoenvironmental Engineering* 129(2):125–135

Ortiz, M. & Popov, E.P. 1982. Plain concrete as a composite material. *Mechanics of Materials* 1:139–150

Villard, P., Jouve, P. & Riou, Y. 1990. Modélisation du compertment mécanique du Texsol. *Bulletin liaison Labo. P et Ch.* 168: 15–27

Voyadijs, G.Z. & Thiagarajan, G. 1995. An anisotropic yield surface model for directionally reinforced metal-matrix composites. *International journal plasticity* 11(8): 867–894

Zhu, Y.T., Zong, G. Manthiram, A. & Eliezer, Z. 1994 Strength analysis of random short-fibre-reinforced metal matrix composite materials. *Journal of material science* 29:6281–6286

Zornberg, J.G. 2002 Discrete framework for equilibrium analysis of fibre-reinforced soil. *Géotechnique* 52(8): 593–604